ably more flattened, with C(17) only 0·58 Å removed from the plane of C(9), C(12), C(16) and C(18). There is considerable evidence of molecular strain in this region of the molecule. In particular, two of the bonds radiating from C(9) [C(9)–C(8) 1·583(6) Å; C(9)–C(17) 1·580(5) Å] are significantly longer than might otherwise be expected for similar bond types in a less restricted environment. For the C(9)–C(8) bond the substituents on both atoms are fully eclipsed, while for the C(9)–C(17) bond, although there is slight staggering, both atoms are fully substituted by relatively bulky groups. Similar lengthening of C sp^3–C sp^3 bonds has been noted in similar molecules where comparable constraints exist (Cameron, Hair, Greengrass & Ramage, 1974; Beisler, Silverton, Penttila, Horn & Fales, 1971; Gilardi, 1972). In the same context, the valency angles about C(9) [100·4→115·5°], C(8) [104·2→114·6°], C(17) [101·7→120·0°] and C(18) [100·2→117·1°] show considerable distortions from tetrahedral values, the smaller angles in general being endocyclic with respect to the fused ring system, while the larger angles are exocyclic. The relative values of the angles are also in accord with those which would be expected to arise both from the restrictions of the cyclic system, and also from the interactions of bulky substituents.

Other dimensions within the molecule compare well with literature values for similar bonding situations. There are no abnormally short intermolecular distances, and the molecular packing would therefore appear to be dominated largely by van der Waals forces.

We (A.F.C. and A.A.F.) thank Imperial Chemical Industries Limited, Pharmaceuticals Division, for financial support.

References

ANANCHENKO, S. N. & TORGOV, I. V. (1959). *Dokl. Akad. Nauk. SSSR*, **127**, 553–556.
BEISLER, J. A., SILVERTON, J. V., PENTTILA, A., HORN, D. H. S. & FALES, H. M. (1971). *J. Amer. Chem. Soc.* **93**, 4850–4855.
CAMERON, A. F., HAIR, N. J., GREENGRASS, C. W. & RAMAGE, R. (1974). *Acta Cryst.* B**30**, 282–289.
DOUGLAS, G. H., GRAVES, J. M. H., HARTLEY, D., HUGHES, G. A., MCLOUGHLIN, B. J., SIDDALL, J. & SMITH, H. (1963). *J. Chem. Soc.* pp. 5072–5094.
GILARDI, R. D. (1972). *Acta Cryst.* B**28**, 742–746.
HUISMAN, H. O. (1968). *Bull. Soc. Chim. Fr.* pp. 13–24.
HUISMAN, H. O. (1971). *Angew. Chem. Int. Ed.* **10**, 450–459.
STEWART, J. H. (1967). Technical Report TR-67-58, Univ. of Maryland.

Acta Cryst. (1974). B**30**, 1927

X-ray Diffraction from Fatty-Acid Multilayers. Significance of Intensity Data in Low-Angle Diffraction

BY W. LESSLAUER

Institute for Pathology, University of Basel, Switzerland

(*Received* 6 *December* 1973; *accepted* 26 *March* 1974)

X-ray diffraction has been recorded from various fatty-acid multilayer systems (barium stearate, barium myristate, magnesium stearate at 0 and 100% relative humidity). The multilayers are treated as simple trial structures for low-angle diffraction experiments with biological membranes. Spacings and intensities of reflexions are analysed. Fourier syntheses calculated with scaled amplitudes of the structure factors provide electron-density functions of the bilayer profiles which are on an absolute scale of electron density.

Introduction

Planar multilamellar systems (multilayers) can be prepared with salts of long-chain fatty acids by the technique of Blodgett (1935). These multilayers are built up by dipping a solid support such as a flat glass plate through a monomolecular film of the fatty acid spread on the surface of an electrolyte solution. Successive monomolecular layers are then transferred onto the support every time it passes through the monomolecular film. The molecules in the multilayer are overturned in every other layer so that a plane of symmetry exists between two neighbouring monolayers. Multilayers, then, consist of a sequence of stacked and parallel bilayers.

The electron density of a multilayer will be called $g(\mathbf{r})$. The normal to the plane of the bilayers is defined as the z axis and the structure will have rotational symmetry and constant radius around z. $g(\mathbf{r})$ in cylindrical coordinates is then

$$g(r,\varphi,z)=u(r)\,.\,\varrho(z)$$

where $u(r)$ is the density function in the bilayer plane. In the following discussion $u(r)$ is assumed to be con-

stant. The one-dimensional electron density function $\varrho(z)$ is given by

$$\varrho(z)=\varrho_0(z)*I_N(z)$$

where $\varrho_0(z)$ refers to one unit cell and $*$ stands for a convolution operation. N is the number of unit cells in the multilayer system. $I_N(z)$ is a one-dimensional finite lattice peak function

$$I_N(z)=s(z)\,.\sum_{h=-\infty}^{\infty}\delta(z-hd)$$

where $\delta(z)$ is a Dirac delta function and $s(z)$ a step function with $s(z)=1$ for $|z|\leq Nd/2$ and $s(z)=0$ for $|z|>Nd/2$. d is the unit-cell dimension in the **z** direction.

Experimental methods

Monomolecular films of stearic and myristic acid were spread on the surface of a $1{\cdot}5\times10^{-4}$ M phosphate buffer (pH 7·5) containing either 10^{-3} M $BaCl_2$ or 10^{-3} M $MgCl_2$. The fatty acids used were of purity better than 99% (Appl. Sci. Lab.). All reagents were of analytical grade. Solvents were redistilled before use.

Multilayers were built up on a silver mirror which was freshly evaporated onto a curved glass slide. Dipping was performed by a motor-driven device. Monomolecular films on the electrolyte solution were kept at constant and high surface pressure during dipping by a moving float (Sher & Chanley, 1955).

X-ray diffraction experiments were performed with a Jarrell–Ash microfocus generator with an adjustable cathode and a focal spot of $1{\cdot}4\times0{\cdot}1$ mm on the anode. The camera was equipped with line-focusing Franks mirror optics and vacuum path. Specimens were kept in a sealed specimen chamber where the relative humidity could be controlled during exposures. High relative humidity (designated 100% r.h.*) was achieved by flushing the specimen chamber with water-vapour-saturated helium. 0% r.h. refers to a condition where P_2O_5 was placed in the evacuated specimen chamber. Experiments were performed at thermostatted room temperature ($29\pm1{\cdot}5$ °C).

Diffraction patterns were recorded on Ilford Industrial G X-ray film. Spacings and integrated intensities of reflexions were measured on densitometer tracings of the diffraction patterns (Joyce–Loebl double-beam microdensitometer MK IIIb). Corrected and normalized intensity data are given as $|F_n|$, where $|F_n(h)|^2=khI(h)$. $I(h)$ is the integrated intensity of reflexion of order h, and $k=1/\sum_h hI(h)$. For scaling factors see below. An additional correction must be applied to the intensity of lamellar reflexions near the origin for absorption phenomena which become apparent from point-focus diffraction patterns.

* r.h.: relative humidity.

Results and analysis

Lamellar reflexions were recorded from multilayers of barium stearate and myristate, and of magnesium stearate (Fig. 1). The number of bilayers, N, in these structures varied from 30–60. The multilayers were kept under atmospheres of either 0 or 100% r.h. during exposures. No difference in the recorded diffraction was noted at the two relative humidities with the barium structures. However, both spacings and relative intensities of the reflexions were found to depend on the relative humidity with magnesium stearate multilayers (Fig. 2). The observed spacings are given in Table 2. From the cell dimensions of the barium myristate and stearate multilayers, the average increment in d per methylene group is about 1·26 Å, which compares reasonably with the value of 1·25 Å observed in the normal form of paraffin crystals (Müller, 1930). The standard variations in d are, however, too large to establish definitely the analogy with the normal form of paraffin crystals. Fourier syntheses $\varrho'(z)=\varrho(z)-\bar{\varrho}$,

$$\varrho'(z)=\frac{2}{d}\sum_{h=1}^{h\max}(\pm)|F(h)|\cos(2\pi zh/d) \qquad (1)$$

can be calculated with the $|F|$ data, provided the correct signs for $|F(h)|$ can be found. From the known chemical composition and the general properties of fatty-acid multilayers (*e.g.* Bücher *et al.*, 1967) there is little doubt about how the correct Fourier map should appear. The dominant criterion is that it must have a flat hydrocarbon core. An intuitive phasing argument, therefore, may be based on a search by trial and error through all solutions for such a flat hydrocarbon core. It is indeed found that for all magnesium and barium stearate multilayers there is only one Fourier synthesis among all independent solutions that gives any extended flat region in $\varrho'(z)$ to be identified as the hydrocarbon core of the bilayer. These solutions which will be corroborated below are given in Fig. 3. They have in addition to the flat hydrocarbon region headgroup peaks and a central trough in the region of the methyl groups (Fig. 3). The values of $\varrho'(z)$ are relative to the average density $\bar{\varrho}$ of the cell. Furthermore, they are on an arbitrary scale. $\bar{\varrho}$ and the correct scaling factors for $|F_n|$ must be derived if the absolute densities of the different regions of $\varrho'(z)$ are to be established. In principle, scaling factors can be calculated from models of the different structures which make use of their known chemical composition (Worthington, 1969). Step-function models are suitable for such calculations. The bilayer profile of the fatty-acid multilayers will be represented by a series of pairwise symmetric step functions $s_j(z)$ of width Δ_j [$s_j(z)=1$ for $|z|\leq\Delta_j/2$, and $s_j(z)=0$ for $|z|>\Delta_j/2$] . $s_j(z)$ will be scaled by the average electron density ϱ_j in the corresponding region of the bilayer and be placed at the proper position ξ_j on the z axis by a convolution with a pair of symmetric delta functions $\delta(z+\xi_j)$ and

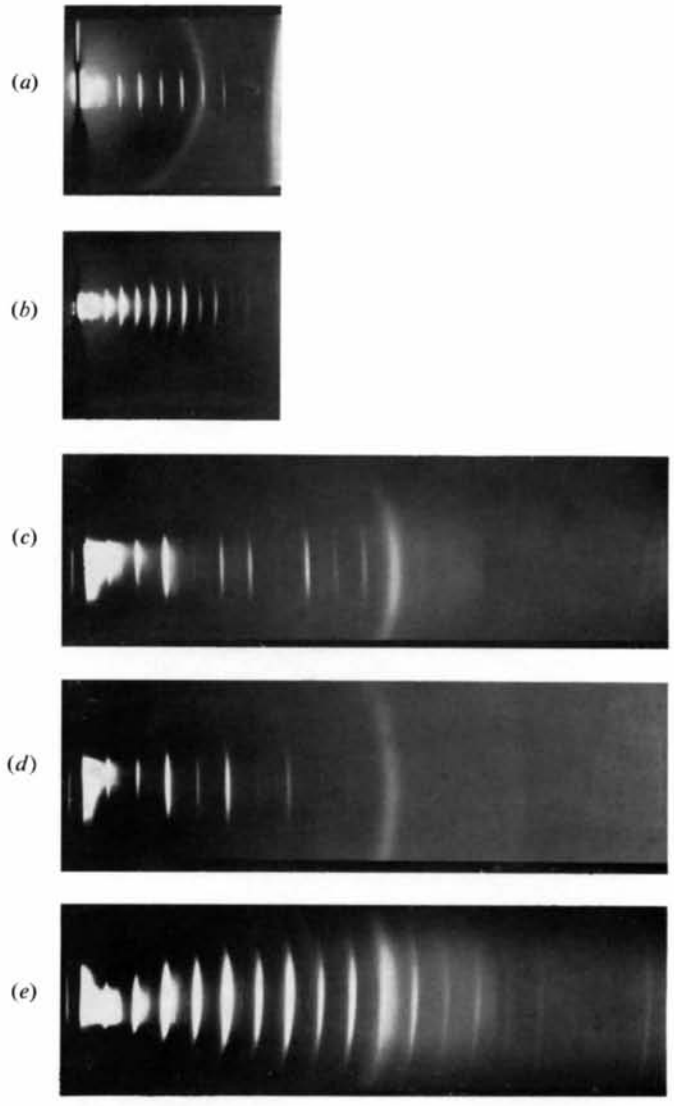

Fig. 1. Examples of X-ray diffraction patterns from different multilayer systems. Ni-filtered Cu $K\alpha$ radiation and cameras with cylindrical cassettes with diameters of 62·5 and 125 mm were used. (Contact prints of the original diffraction patterns.) (*a*) Barium myristate multilayer, $N=40$, cassette of 62·5 mm. (*b*) Barium stearate multilayer, $N=60$, cassette of 62·5 mm. (*c*) Magnesium stearate multilayer at 100% r.h., $N=43$, cassette of 125 mm. (*d*) Magnesium stearate multilayer at 0% r.h., $N=43$, cassette of 125 mm. (*e*) Barium stearate multilayer, $N=60$, cassette of 125 mm.

[*To face p.* 1928

$\delta(z-\xi_j)$. The bilayer profile then can be described (see Fig. 4) by

$$\varrho(z) \simeq \sum_j \varrho_j \,.\, s_j(z) * [\delta(z+\xi_j)+\delta(z-\xi_j)] \,. \qquad (2)$$

The transform for this model is, with $s_j(z) \Leftrightarrow \Delta_j \mathrm{sinc}(\pi\Delta_j Z)$ and $[\delta(z+\xi_j)+\delta(z-\xi_j)] \Leftrightarrow 2\cos(\pi\xi_j Z)$,

$$F(Z) \simeq 2 \sum_j \varrho_j \Delta_j \,\mathrm{sinc}\,(\pi\Delta_j Z)\cos(\pi\xi_j Z) \,. \qquad (3)$$

An expression for the scaling factor for the experimental $|F_n|^2$ which will be called κ can be derived by using Parseval's theorem

$$\int_{-\infty}^{\infty} |F_{\mathrm{abs}}(Z)|^2 \mathrm{d}Z = \int_{-d/2}^{+d/2} \varrho^2(z)\mathrm{d}z$$

where $|F_{\mathrm{abs}}|^2$ is on an absolute scale. With

$$\int_{-\infty}^{\infty} |F_{\mathrm{abs}}(Z)|^2 \mathrm{d}Z \simeq \frac{1}{d}|F_{\mathrm{abs}}(0)|^2 + \kappa \frac{2}{d} \sum_{h=1}^{h\max} |F(h)|^2$$

one obtains

$$\kappa \sum_{h\max}^{h=1} |F_n(h)|^2 = \frac{d}{2}\left[\int_{-d/2}^{d/2} \varrho^2(z)\mathrm{d}z - \frac{1}{d}|F_{\mathrm{abs}}(0)|^2\right] . \qquad (4)$$

The scaling factor κ then can be evaluated for the step function model of Fig. 4. It becomes

$$\kappa \frac{1}{d} \sum_{h=1}^{h\max} |F_n(h)|^2 = (\varrho_3-\varrho_2)^2\Delta_2 + (\varrho_3-\varrho_1)^2\Delta_1$$
$$- 1/\Delta_{1,2,3}\,[(\varrho_3-\varrho_2)\Delta_{1,2} + (\varrho_2-\varrho_1)\Delta_1]^2$$
$$+ \Delta_{1,2,3}/\Delta_{1,2,3,4}(\bar{\varrho}_{1,2,3}-\varrho_4)^2\Delta_4 \qquad (5)$$

where

$$\Delta_{1,2,\ldots} = \Delta_1 + \Delta_2 + \ldots$$

and

$$\bar{\varrho}_{1,2,3} = (\varrho_1\Delta_1 + \varrho_2\Delta_2 + \varrho_3\Delta_3)/\Delta_{1,2,3} \,.$$

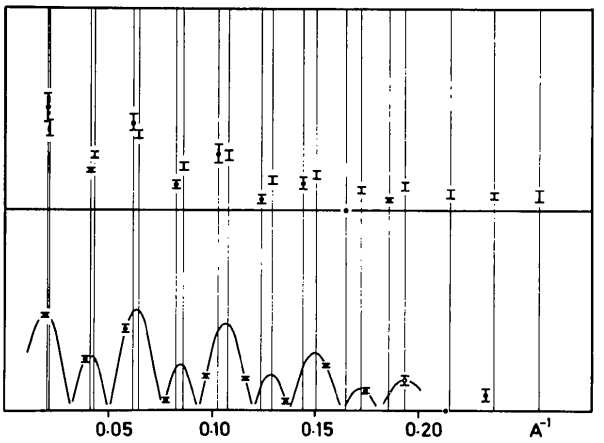

Fig. 2. Normalized amplitudes of the structure factor $|F_n|$ with standard variations. Normalization factors are obtained by setting the sum of the corrected observed intensities equal to 1·0. In the to phalf, $|F_n|$ for the barium stearate (○) and the magnesium stearate multilayer at 0% r.h. (●) are given. In the lower half are $|F_n|$ and the reconstructed continuous transform for the magnesium stearate structure at 100% r.h.

Approximate values for the ϱ_j and Δ_j must be chosen from model considerations in order to compute κ. These parameters are derived for the headgroup regions in the following way. Diffraction from magnesium multilayers is affected by the relative humidity, whereas that from barium multilayers is not. Therefore, it is concluded that barium ions are incorporated in the multilayer in non-hydrated form, but that magnesium ions have coordinated water molecules when they are incorporated into the multilayer structure, which are removed at 0% r.h. This conclusion is supported also by a comparison of the ionic radii and the heats of hydration of Ba^{2+} and Mg^{2+} (Voet, 1936). In hydrated magnesium chloride crystals (Andress & Gundermann, 1934) six coordinated water molecules are arranged octahedrally around the magnesium ion. In the multilayer all places in the coordination sphere of the magnesium ion are not necessarily occupied by water molecules even at 100% r.h. It is, however, assumed that $Mg(H_2O)_6^{3+}$ and Mg^{2+} are the counterions in the magnesium multilayers at 100% and at 0% r.h. The headgroup per chain then is made up from the electrons of half a counterion and from those of the carboxyl group. An approximate value for Δ_3 is derived from the radius of the largest ion or atom in the headgroup. Similar considerations lead to approximate values for the other Δ_j and ϱ_j (Table 1). The resulting scaling factors κ are 99·1, 76·7, and 19·4 for the barium, magnesium (100% r.h.) and magnesium (0% r.h.) stearate multilayers. The functions $\varrho(z)$ in Fig. 3 were calculated with the thus scaled $|F_n|$ data and were placed with the derived average density $\bar{\varrho}$ of the cell on the same absolute scale indicated in the figure. The flat regions assigned to the region of the methylene groups of all three structures then superpose with reasonable accuracy at a density of about 0·28–0·31 e $Å^{-3}$. Such electron densities are to be expected from methylene regions of hydrocarbon cores. The density of methylene regions in paraffin crystals of the normal form can be as high as 0·34 (Müller, 1932). In a phospholipid bilayer a value of 0·28 was observed (Lesslauer, Slotboom & de Haas, 1973). From monomo-

Table 1. *Model parameters in the scaling procedure* (Δ_j *in* Å, ϱ_j *in* e$Å^{-3}$)

	Δ_1	ϱ_1	Δ_2	ϱ_2	Δ_3	ϱ_3	Δ_4	ϱ_4
Barium stearate	2·6	0·13	19·25	0·28	1·5	1·50	0	
Magnesium stearate, 0% r.h.	2·6	0·13	19·25	0·28	1·5	0·77	0·9	~0·33
Magnesium stearate, 100% r.h.	2·6	0·13	19·25	0·28	2·2	1·10	1·2	~0·33

lecular film studies values of about 0·30 are suggested (Adam, 1930). The scaling procedure applied also assigns for the headgroup peaks and the region of the methyl groups densities which agree with reasonable accuracy with the absolute densities in the structure.

Table 2. *Unit-cell dimensions of the various structures (with standard variation)*

Multilayer	d (Å)
Barium stearate	46·3 ± 0·4
Barium myristate	36·2 ± 1·1
Magnesium stearate (0% r.h.)	48·5 ± 0·3
Magnesium stearate (100% r.h.)	51·6 ± 0·8

Discussion

The phasing argument used may seem arbitrary, although it results in a physically reasonable scaled $\varrho(z)$. There are, however, independent arguments which support the solutions given in Fig. 3. Multilayers with any number of bilayers up to around 100 can be easily prepared by the Blodgett procedure. Therefore, diffraction from systems with only a few cells can be recorded. Under these conditions an interference function with peaks of finite width samples $|F|^2$. Following the theories of Hosemann & Bagchi (1962) the autocorrelation function of the structure can then be calculated and $\varrho(z)$ obtained directly by a deconvolution of the autocorrelation function. Such computations lead to results which are consistent with the above phasing argument (Lesslauer, 1971; Lesslauer & Blasie, 1972).

Furthermore, a tentative phasing argument might be based on the 'swelling' behaviour of the magnesium structures. Fig. 3 shows that the basic argument of swelling experiments does not hold accurately for the magnesium multilayers at 0 and 100% r.h. The 'swelling' is not restricted to a removal of water from an aqueous layer. Rather the structure of the two bilayers is different with respect to the headgroup and methyl regions. This is equivalent to the observation (Fig. 2) that no arbitrary scaling factor can be found which will fit all $|F_n|$ of the magnesium structure at 0% r.h. exactly on the reconstructed transform for the magnesium stearate bilayer at 100% r.h. (Shannon, 1949; Sayre, 1952). The two magnesium structures are, however, of the same type. The close relation of the continuous transform of the hydrated structure and the general trend of $|F_n(h)|$ of the dehydrated structure is seen perhaps most clearly in the region of the missing eighth order of the dehydrated structure where the continuous transform also has a zero. Similarly, Fig. 2 suggests also that the barium stearate bilayer has a transform of the same type.

The physical reasons for the difference in the headgroup peaks of the two magnesium structures are obvious. It is noteworthy, however, that width and depth of the methyl trough in $\varrho(z)$ also vary with the water content in the headgroup of the structure. This feature is most probably not due to limited resolution of the Fourier maps. The highest frequency term in the Fourier sum has a period of about 5·4 Å at 0% and about 4·3 Å at 100% r.h. The width of the methyl trough, therefore, should be above resolution limit. It is likely that the precise arrangement of the chains depends on the water content of the system (*e.g.* Luzzati, 1968).

It is obvious that the exact values of the scaling factors κ depend on the choice of the model parameters Δ_j and ϱ_j. More accurate scaling factors might be obtained, in principle, if the model parameters in equation (5) were readjusted in an iterative process to the

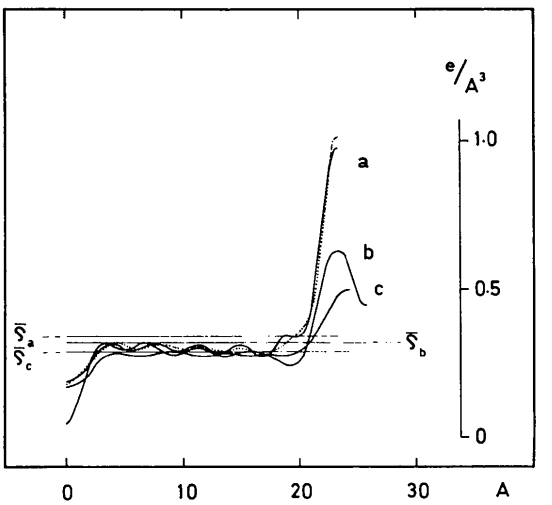

Fig. 3. Electron-density function of the half cell of (*a*) the barium stearate, and the magnesium stearate bilayer at (*b*) 100% and (*c*) 0% r.h. (*a*) and (*b*) are calculated with 12 reflexions, (*c*) with 9 reflexions. A higher resolution density function for the barium stearate bilayer is included (17 reflexions, dotted line). The Fourier syntheses in the figure were calculated with scaled $|F_n|$ and were placed with the respective average densities $\bar{\varrho}_a$, $\bar{\varrho}_b$ and $\bar{\varrho}_c$ on the same absolute scale indicated in the figure.

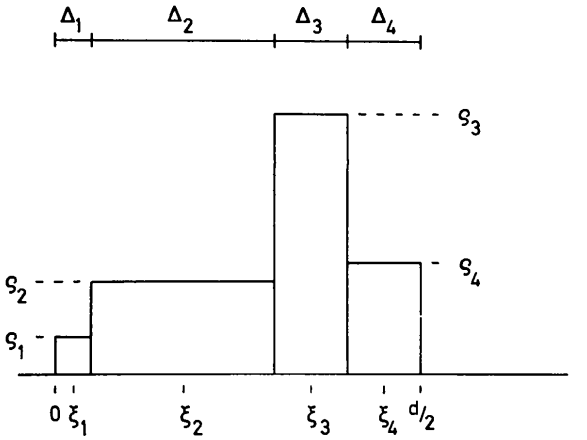

Fig. 4. Step-function model of the bilayer profile used in the scaling procedure.

calculated scaled $\varrho(z)$, until a constant value for κ is obtained. The fit of the absolute scale would then depend only on the accuracy of $\bar{\varrho}$. The resolution of $\varrho(z)$ in Fig. 3 is, however, too low and $\bar{\varrho}$ is not known accurately enough to make such a parameter variation successful. It will suffice that physically reasonable Δ_j and ϱ_j in equation (5) result in scaling factors which put $\varrho(z)$ on a physically reasonable absolute scale of electron density. The effect of increased resolution in $\varrho(z)$ becomes apparent when additional reflexions are added into the Fourier map. A higher resolution $\varrho(z)$ for the barium stearate bilayer is included in Fig. 3 (dotted line). Five additional orders were used. They were phased under the assumption that the flat hydrocarbon core should be preserved. It follows that the main effect of increased resolution is a sharpening of the headgroup peaks. For this reason it is not to be expected that a parameter variation for the κ will be successful if they are readjusted to the calculated $\varrho(z)$ at limited resolution.

Conclusions

Low-angle X-ray diffraction has proved a suitable method for obtaining information on the molecular structure of liquid-crystalline systems and of biological membranes. A significant advantage in the study of biological membranes compared with microscopic techniques is that no fixation, staining and dehydration of materials is needed in order to obtain diffraction. It is essential to demonstrate, however, that not only the spacings but also the intensities of the recorded reflexions contain reliable information on the molecular structure of the system under investigation, which can be analysed quantitatively. This can be done only by investigating a simple trial structure which has certain analogies with the more complex systems of biological membranes. The suitability of a model is determined among other things by the method by which a structure is to be studied. From the methodological point of view fatty-acid multilayers are a model for biological membranes, because they contain elements which also determine the diffraction from biological membranes.

The analysis of intensity data from fatty-acid multilayers does lead to scaled electron-density profiles which are physically reasonable, because they fit the known chemical composition of the structure. Flat hydrocarbon cores with a width of approximately 19 Å and a density of 0·28–0·30 e $Å^{-3}$ in the methylene regions are observed. Width and height of the headgroup peaks in the barium and the two magnesium structures correspond quite accurately with the number of electrons in the respective headgroups. The density in the methyl region of the water-containing magnesium structure appears to be significantly lower than in the other bilayers.

Diffraction experiments were performed during the author's stay at the Department of Biophysics and Physical Biochemistry of the University of Pennsylvania, Philadelphia. During that time he was supported by funds from the Johnson Research Foundation. Computations were done on a PDP 9 (Inst. Phys. Chem., University of Basel). The microdensitometer was on loan from CIBA-Geigy AG (Basel). The work was supported in part by the Schweizer Nationalfonds (3.8850.72).

References

ADAM, N. K. (1930). *The Physics and Chemistry of Surfaces*, pp. 25–91. Oxford: Clarendon Press.

ANDRESS, K. R. & GUNDERMANN, J. (1934). *Z. Kristallogr.* **87**, 345–369.

BLODGETT, K. B. (1935). *J. Amer. Chem. Soc.* **57**, 1007–1022.

BÜCHER, H., DREXHAGE, K. H., FLECK, M., KUHN, H., MÖBIUS, D., SCHÄFER, F. P., SONDERMANN, J., SPERLING, W., TILLMANN, P. & WIEGAND, J. (1967). *Mol. Cryst.* **2**, 199–230.

HOSEMANN, R. & BAGCHI, S. N. (1962). *Direct Analysis of Diffraction by Matter*, pp. 120–131. Amsterdam: North Holland.

I ESSLAUER, W. (1971). *Proc. I. Eur. Biophys. Congress Baden/Vienna*, Vol. IV, pp. 425–429.

LESSLAUER, W. & BLASIE, J. K. (1972). *Biophys. J.* **12**, 175–190.

LESSLAUER, W., SLOTBOOM, A. J. & DE HAAS, G. H. (1973). *Chem. Phys. Lipids*, **11**, 181–195.

LUZZATI, V. (1968). In *Biological Membranes*, edited by D. CHAPMAN, pp. 71–123. London: Academic Press.

MÜLLER, A. (1930). *Proc. Roy. Soc.* A**127**, 417–430.

MÜLLER, A. (1932). *Proc. Roy. Soc.* A**138**, 514–530.

SAYRE, D. (1952). *Acta Cryst.* **5**, 843.

SHANNON, C. E. (1949). *Proc. Inst. Radio Engrs. N.Y.* **37**, 10–21.

SHER, I. H. & CHANLEY, I. D. (1955). *Rev. Sci. Instrum.* **26**, 266–268.

VOET, A. (1936). *Trans. Faraday Soc.* **32**, 1301–1304.

WORTHINGTON, C. R. (1969). *Biophys. J.* **9**, 222–234.